Available online at www.sciencedirect.com
SCIENCE DIRECT
Polymer 46 (2005) 5541–5549
polymer
www.elsevier.com/locate/polymer

Light scattering and viscoelasticity study of poly(vinyl alcohol)–borax aqueous solutions and gels

Hsiu-Li Lin[a], Yuan-Feng Liu[a], T. Leon Yu[a,*], Wen-Horng Liu[a], Syang-Peng Rwei[b]

[a]*Department of Chemical Engineering and Materials Science, Yaun Ze University, Nei-Li, Taoyuan 32026, Taiwan, ROC*
[b]*Institute of Organic and Polymeric Materials, National Taipei University of Technology, Taipei 10021, Taiwan, ROC*

Received 22 October 2004; received in revised form 13 April 2005; accepted 25 April 2005
Available online 26 May 2005

Abstract

Poly(vinyl alcohol)–borate (PVA–borate) aqueous solutions properties with PVA concentrations ranging from 2 to 60 g/L and borax concentrations of 0.0 and 0.2 M were investigated at room temperature using static and dynamic light scattering (SLS and DLS), and dynamic viscoelasticity measurements. Light scattering and viscoelasticity data revealed that all the PVA–borate aqueous systems, except those with [PVA] ≥ 40 g/L and [borax] = 0.2 M, behaved as solutions. For PVA–borate aqueous systems with [PVA] ≥ 40 g/L and [borax] = 0.2 M, light scattering data revealed that these systems behaved like gels, but viscoelasticity data showed that these systems were in flow states. The experimental data suggest that PVA–borate aqueous systems with [PVA] ≥ 40 g/L and [borax] = 0.2 M are thermoreversible gels with finite equilibrium life time of thermoreversible borate–PVA di-diol crosslinks. The thermoreversible crosslinks can be observed by the non-perturbing light scattering technique but not by the pertubing rheometric method. These results indicate the advantage of light scattering relative to rheometers for studying the physical or reversible crosslink gels.

Keywords: Poly(vinyl alcohol); Light scattering; Viscoelasticity

1. Introduction

Studies of polymer–ion complexes have been continued vigorously in recent years due to their wide range of application. Poly(vinyl alcohol) (PVA) is one of the most typical capable of polymer–ion complexation [1]. PVA has several unique features: it is water soluble, crystallizable, capable of hydrogen bonding, and forms ion complexes with various ions, such as borate [2,3], vanadate [4], and Congo red [5,6]. PVA–borate complexation reversible gels have received much attention because these materials have attractive physical chemical properties and industrial interest, especially the application in oil industry as fracturing fluids [7]. The structures and properties of PVA–borate complex aqueous solutions have been studied extensively in recent years [8,9]. The mechanism of the crosslink reaction of borate ion with PVA is believed to be a so-called 'di-diol' complexation, which is formed between two diol units and one borate ion [10,11].

The PVA–borate crosslinking mechanism is divided into two reactions, i.e. monodiol complexation (reaction (1)) and a crosslink reaction (reaction (2)) as shown by the following equations: [11,12]

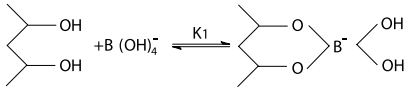

(1)

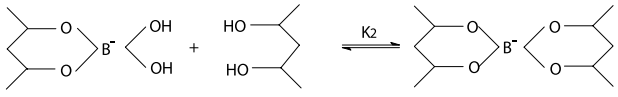

(2)

Once a borate ion is attached to a polymer chain (reaction (1)), the polymer chain behaves as a polyelectrolyte unless the borate ion is removed from the chain. In this case, a significant contribution of electrostatic repulsion between monodiol units is expected, resulting in an expansion of the individual polymer chains.

In dilute polymer solutions, the size of PVA–borate ion

* Corresponding author. Tel.: +886 3 4638800x2553; fax: +886 3 4559373.
E-mail address: cetlyu@saturn.yzu.edu.tw (T.L. Yu).

0032-3861/$ - see front matter © 2005 Elsevier Ltd. All rights reserved.
doi:10.1016/j.polymer.2005.04.074

complex is lowered due to intra-molecular crosslink formation through reaction (2), and an aggregation of polymer molecules may also be expected if the polymer–polymer attractive interaction is greater than the polymer–solvent interaction. The chain dimension and the stability of PVA–borate complex system are ruled by electrostatic repulsion and intra-molecular crosslink.

In semidilute polymer solutions, both intra- and inter-molecular crosslink through reaction (2) may happen, and a gelation of PVA–borate complex is expected. Sol–gel transition and re-entrant behavior of PVA–borate gel and solutions has been studied extensively in recent years [11–14]. Koike et al. [15] studied PVA–borax aqueous solutions with PVA concentration ranged from 1.5 to 2.0 wt%, using dynamic light scattering (DLS) and dynamic viscoelasticity measurements. Since their PVA concentrations were slightly higher than overlap concentration, the samples behaved like weak gels. DLS revealed two relaxation modes with the slow mode relaxation time (τ_s) being close to the mechanical relaxation time obtained from viscoelasticity measurement.

Experiment and theoretical analyses have been developed expressions for the frequency (ω) dependence of storage modulus (G') and loss modulus (G'') at the gel point, using the fractal-scaling concept to define 'gel'. The relations of G' and G'' with ω are shown in Eqs. (3) and (4): [16–18]

$$G'(\omega) = A\omega^{n'} \tag{3}$$

$$G''(\omega) = B\omega^{n''} \tag{4}$$

Where n' and n'' are the exponents of storage and loss modulus, respectively; and A and B are related to the material strength factor of the gel [16]. According to Winter et al. [16–18], $n' = n''$ (critical exponent) at sol–gel transition. The exponents n' and n'' are determined by the fractal dimension of the network, the stoichiometry of the gel [19], and the strength of the hydrodynamic interaction between the polymer chain segments [20]. At gel point the storage modulus $G'(\omega)$ and loss modulus $G''(\omega)$ are congruent over the whole spectrum frequencies.

In literature, very few papers were reported on the viscoelastic properties of PVA–borax aqueous solutions. Cheng and Rodriguez [21], using a test-tube torsion pendulum and an air-bearing torsion pendulum, measured the dynamic mechanical properties of PVA–boric acid aqueous solutions in the presence of NaOH. They reported that at a fixed PVA concentration, the storage modulus increases with increasing borate and NaOH concentration, and reached a plateau value while borate and NaOH concentrations are higher than a critical concentration. Robb and Smeulders [22] also studied the rheological properties of PVA/ borate aqueous gels. However, no critical exponents with $n' = n''$ at sol–gel transition was reported by both Cheng and Robb groups. Kjoniksen and Nystrom [23] studied the evolution of viscoelasticity during gelation of semi-dilute solutions of PVA in the presence of permanent chemical cross-linker (i.e. glutaraldehyde). Critical exponents with $n' = n''$ was observed at sol–gel transition. They also found that the exponents n' and n'' at sol–gel transition decrease monotonically with increasing PVA concentration, and, especially at a low PVA concentration, n' and n'' falls off with increasing cross-linking density at a given PVA concentration. It is obvious that the main difference between these two systems is that PVA–borate aqueous system is a thermoreversible equilibrium gels and the PVA–glutaraldehyde aqueous system is a permanent chemical crosslink gels. The crosslink of PVA–borate system has a finite lifetime (τ_{life}) while that of PVA–glutaraldehyde system has an infinite τ_{life}.

It is well known that borax (or sodium tetraborate, $Na_2B_4O_7$) is a good buffer. At low borax concentrations in water, it is totally dissociated into equal quantities of boric acid ($B(OH)_3$), borate ion ($B(OH)_4^-$), and Na^+ [9]. The borate ions and PVA molecules form complexes, which induce electrostatic charges on the polymeric chains. The Na^+ ions have shielding effect on the charges of polymer chains. Thus, the conformation of the polymer chains is a consequence of the balance of excluded volume of the polymers, the electrostatic repulsion among the charged complexes bound on polymeric chains, and the shielding effect of free Na^+ ions on the charged complexes.

In the present work, we report data from static and dynamic light scattering (SLS and DLS), and dynamic viscoelastic measurements of PVA–borax aqueous solutions with PVA concentrations ranging from 2 to 60 g/L and borax concentrations of 0.0 and 0.2 M at 25 °C. Since PVA is not easily to be dissolved at room temperature, in present work, the PVA aqueous and PVA–borax aqueous solutions were mixed and dissolved at 80–90°C then cooled ambiently at room temperature. The critical concentrations (C^*) at 25 and 80 °C calculated from inverse intrinsic viscosity, i.e. $C^* = 1/[\eta]$, are 15.0 and 14.2 g/L, respectively. The PVA–borax complexation reactions (1) and (2) are thermo-equilibrium reactions [2]. When preparaing PVA and PVA–borax aqueous solutions with [PVA] > 15 g/L at 80–90 °C, the PVA molecular chains may overlap and entangled with each other, but few PVA–borax crosslink reactions (1) and (2) happened. However, as solutions were cooled to room temperature, the PVA molecules may aggregate through –OH hydrogen bond and PVA–borate complexation crosslink reactions (1) and (2) to form larger particles or thermo-reversible gels. Light scattering and viscoelasticity measurements were performed at 25 °C, the data revealed that all the PVA–borax aqueous systems, except those with [PVA] ≥ 40 g/L and [borax] = 0.2 M, behave as solutions. For PVA–borax aqueous solutions with [PVA] ≥ 40 g/L and [borax] = 0.2 M, light scattering data revealed that these systems behave like gels, but viscoelasticity data showed that these solutions were in flow states. These results suggest a weak gel behavior of PVA–borax aqueous

solutions with [PVA] ≥ 40 g/L and [borax] = 0.2 M. The gel behavior can be observed by a non-pertubing light scattering technique, but not by a pertubing reheometric method. The experimental results show the advantage of non-perturbing nature of light scattering relative to perturbing rheometers for studying the physical or reversible crosslink gels.

2. Experimental

2.1. Materials

2.1.1. Poly(vinyl alcohol) (PVA) (99% hydrolysis, $M_w = 1.1 \times 10^5$, Aldrich Chemical Co.)

It was dissolved in an *n*-propanol–water system at 80–90 °C and diluted to ~1 wt%. The diluted solution was cooled ambiently at room temperature and filtered through a Millipore HWAP 02500 filter (0.45 μm) to remove dust. PVA was then recovered by re-precipitation with acetone to remove any lower molecular weight species. Before mixed into PVA solution, acetone was filtered through a Millipore HLFP 02500 filter (0.5 μm) to remove any dust in the solvent. The precipitated PVA was kept in a clean glass vessel capped with a piece of Millipore AAWP 02500 filter (1.0 μm) and dried under vacuum for 1 week at 60 °C to remove residue solvent.

2.1.2. Borax (sodium tetraborate, $Na_2B_4O_7$, Riedel-de Haen Co.)

It was dried at 120 °C under reduced pressure for one day before sample preparation.

2.1.3. Preparation of PVA–borax–water solutions

PVA–borax–water solutions with PVA concentrations ranging from 2 to 60 g/L and borax concentrations of 0.0 and 0.20 M were prepared by dissolving PVA into pure water and 0.10 and 0.20 M borax–water solutions in light scattering testing tubes. In order to avoid contamination by dust, the light scattering testing tubes containing solution mixtures were sealed by flame. The sealed testing tubes were then stirred and heated at 80–90 °C for at least 12 h to get homogeneous solutions and then they were cooled ambiently at room temperature at least two days before DLS and dynamic viscoelasticity measurements. Before mixing, pure water and borax–water solutions were filtered through a Millipore HWAP 02500 filter (0.45 μm) and PVA was purified as described in Section 2.1.1.

2.2. Dynamic light scattering (DLS)

The quasi-elastic light scattering was measured with a 256-channel autocorrelator (Brookhaven Co., model BI9000). The laser was a He–Ne ion (633 nm, operated at 20 mW, Spectra Physics model). The experiments were carried out at 25 °C with scattering angles of 30, 45, 60, 90, and 120°. Intensity correlation functions $g^{(2)}(t)$ were obtained from experiments. Most of the experiments were carried out with a measuring time around 3–7 h. For PVA–borax aqueous solutions with [PVA] ≥ 50 g/L, the measuring time were around 12 h till the convergence of long sample time data points were obtained. A heterodyne data analysis method [24–26] was used to calculate field correlation function $g^{(1)}(t)$ from $g^{(2)}(t)$:

$$g^2(t) = 1 + \beta\{2X(1-X)g^{(1)}(t) + X^2[g^{(1)}(t)]^2\} \quad (5)$$

Where X is the homodyne ratio and β the instrumental parameter. X can be obtained from Eq. (6):

$$X = \frac{[1 - [1 + \beta - g^{(2)}(0)]^{1/2}]}{\beta^{1/2}} \quad (6)$$

where $g^{(2)}(0)$ is the value of $g^{(2)}(t)$ at $t \to 0$, and β can be obtained from the initial amplitude, $g^{(2)}(0)$, of polystyrene latex measurements [26]. In this study the β value is around 0.90. The calculation of relaxation times distribution $A(\tau)$ will be discussed in Section 3.

2.3. Dynamic viscoelasticity measurements

2.3.1. High viscosity solutions

Dynamic viscoelasticity $G'(\omega)$ and $G''(\omega)$ measurements were carried out under 5% strain at 25 °C with a cone and plate geometry rheometer (Rheometric Inc., RDS-7000, plate diameter 50 mm, cone angle 0.04 rad).

2.3.2. Low viscosity solutions

An oscillatory flow rheometer (Vilastic VE system, Vilastic Scientific Inc., Austin, TX, USA) with a cylindrical tube of length 6.115 cm and inner diameter 0.0513 cm was used for dynamic viscoelasticity $G'(\omega)$ and $G''(\omega)$ measurements. The measurements were carried at 25 °C.

3. Results and discussion

The polarized (V_v) DLS measurements for PVA–borax aqueous solutions were made at 25 °C. Before each measurement, the sample was kept at the experimental temperature at least 2 days to let the reaction of PVA and borax reach equilibrium. The field correlation functions $g^{(1)}(t)$ obtained at a scattering angle $\theta = 90°$ for PVA aqueous solutions with various PVA concentrations and 0.0 and 0.20 M borax are shown in Figs. 1 and 2, respectively. For all the PVA aqueous solutions mixing with 0.0 M borax (PVA–0 M borax) and 0.2 M borax (PVA–0.2 M borax) aqueous solutions with [PVA] ≤ 20 g/L, an inverse Laplace transformation (ILT) was made from $g^{(1)}(t)$ to obtain the distribution of relaxation times by using CONTIN software [27]. The relaxation time distributions (i.e. $\tau A(\tau)$ vs. $\log \tau$) obtained using CONTIN analyses are also shown Figs. 1 and 2.

The $g^{(1)}(t)$ data for PVA–0.2 M borax aqueous systems

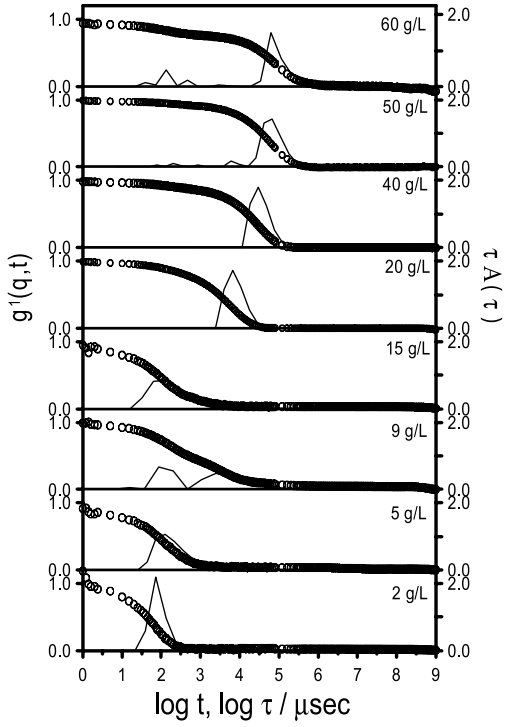

Fig. 1. Field correlation functions $g^{(1)}(t)$ (open circle) and their relaxation time distributions $\tau A(\tau)$ (full line) obtain from CONTIN analysis at a scattering angle $\theta = 90°$ for various concentrations of PVA aqueous solutions.

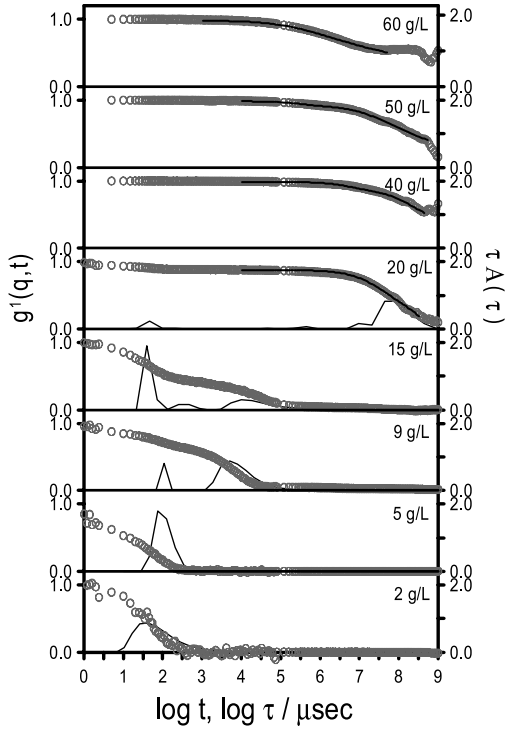

Fig. 2. Field correlation functions $g^{(1)}(t)$ (open circle) at a scattering angle $\theta = 90°$ for various concentrations of PVA aqueous solutions mixed with 0.2 M borax. The relaxation time distributions $\tau A(\tau)$ obtained from CONTIN analysis (full line) are shown for [PVA] $\leq$ 20 g/L and the curves fitted with Eq. (7) (full line) are shown for [PVA] $\geq$ 20 g/L.

with [PVA] $\geq$ 40 g/L show long time tails not reaching the base line (Fig. 2), indicating a fraction of fluctuation becomes frozen-in, which is similar to the $g^{(1)}(t)$ data of other gel systems reported in literature such as PVA–glutaraldehyde aqueous [28], Tamarind Gum–Na_2SO_4–NaN_3 aqueous [29], exopolysaccharide–NaCl aqueous [30], and schizophyllan (a fungal polysaccharice)-D-sorbitol aqueous [31] systems. In latter sections more evidences of gel-like behavior (Fig. 6) for systems with [PVA] $\geq$ 40 g/L and [borax] = 0.2 M will be shown. It has been shown that long time tails of $g^{(1)}(t)$ data of gels can be well fitted by Eq. (7), which is a power-law function [32,33].

$$g^{(1)}(t) = A\left[1 + \left(\frac{t}{\tau}\right)\right]^{-b} \quad \text{for gels} \tag{7}$$

In Eq. (7), A is an adjustable constant, τ the characteristic relaxation time, and the exponent b ($0.5 \geq b \geq 0$) relating to the fractal dimension d of scattered photons by $b = (1-d)/2$ with $1 > d > 0$. The curves for $g^{(1)}(t)$ fitted with Eq. (7), are shown in Fig. 2 for PVA–0.2 M borax aqueous systems with [PVA] $\geq$ 40 g/L, and no relaxation times distributions $A(\tau)$ obtained from CONTIN analysis are shown for these systems. The PVA–0.2 M borax aqueous solution with [PVA] = 20 g/L is a system near the sol–gel transition, both its relaxation time distribution obtained from CONTIN analysis and fitting curve using Eq. (7) are shown in Fig. 2. The parameters A, τ, and b of Eq. (7) for PVA–0.2 M borax aqueous syatems with [PVA] $\geq$ 20 g/L are summarized in Table 1.

As mentioned in Section 1, PVA and PVA–borax aqueous solutions were prepared at 80–90 °C to form homogeneous solutions then cooled to room temperature. During cooling, the association among PVA molecules through OH–hydrogen bond and PVA–borate crosslink reactions (1) and (2) to form bigger aggregation particles may happen. As shown in Fig. 1 the relaxation time of PVA increases with PVA concentration, indicating that there is an aggregation among PVA molecules. For PVA–0.2 M borax aqueous solutions (Fig. 2), the relaxation time of PVA–borate complex increases as PVA concentration increases from 2 to 20 g/L. As PVA concentration is higher than 40 g/L, a gel-like behavior of these systems is observed and the relaxation time τ decreased as PVA concentration is increased from 40 to 60 g/L (Table 1). The PVA molecules may crosslink through –OH hydrogen bond and borate–PVA di-diol complexation (i.e. reaction (2)).

Two groups of relaxation modes were observed in these correlation functions, i.e. fast modes with relaxation times (τ_f) located around 10^1–10^3 μs and slow modes with relaxation times (τ_s) located at a time longer than 10^3 μs. The slow relaxation time τ_s and slow mode amplitude A_s increase with increasing PVA concentration. For PVA–0 M borax aqueous solutions, Fig. 1 shows that sizes of slow mode particles increase with increasing PVA concentration,

Table 1
Curve fitting parameters of Eq. (7) for PVA–borax aqueous gels with [PVA]≥20 g/L and [borax]=0.2 M

[PVA]	20 g/L	40 g/L	50 g/L	60 g/L
A	0.930±0.010	0.942±0.06	0.955±0.003	0.971±0.007
τ (μs)	(3.05±0.10)×10^7	(1.40±0.22)×10^8	(1.65±0.11)×10^7	(1.92±0.23)×10^5
b	0.53±0.03	0.37±0.04	0.23±0.01	0.11±0.01
d	0.0	0.26	0.54	0.78

indicating more molecules aggregate and form big particles. The aggregation of polymer chains into larger particles may reduce the polymers occupied space in the solutions and these PVA big aggregated particles may not overlap with each other at room temperature. Thus the motions of aggregated particles behave like in dilute solutions. As will be shown later in Figs. 4 and 5, DLS intra-particle motions of these particles were also observed. Fig. 1 also shows that the value of fast mode τ_f is almost independent of PVA concentration, indicating that τ_f corresponds to the relaxation times of unassociated PVA molecules. Fig. 1 also shows that as [PVA]≤5 g/L only fast relaxation mode ($\tau_f < 10^3$ μs) is observed, indicating that few PVA molecular aggregations occur. However, as PVA concentration is close to C^* (9 g/L≤[PVA]≤20 g/L), Fig. 1 shows the slow relaxation modes ($\tau_s > 10^3$ μs) appear and the τ of relaxation modes distributes from 10^1 to 10^5 μs in DLS data, indicating that some of the PVA molecules aggregate through –OH inter-molecular hydrogen bonding. As [PVA]≥40 g/L, slow relaxation mode dominates DLS relaxations, indicating that most of the PVA molecules aggregate and form larger particles. The sizes of the aggregated particles increase with increasing PVA concentration.

While 0.2 M borax is mixed into PVA aqueous solutions, in the dilute regime (i.e. [PVA]≤5 g/L) borate–PVA diol (Eq. (1)) and borate–PVA di-diol intra-molecular crosslink reactions (Eqs. (1) and (2)) dominate the reactions between borate and PVA-diol, and Fig. 2 shows that only fast relaxation mode is observed in DLS data. Fig. 2 also shows that for [PVA]≤5 g/L, the relaxation times of PVA–0.2 M borax aqueous solutions are shorter than those of PVA–0 M borax aqueous solutions while PVA is at a fixed concentration (Fig. 1), indicating a reduction of PVA molecular chains sizes while the solutions are mixed with borax. One of the reasons for the reduction of PVA molecular sizes while borax is mixed into PVA aqueous solutions is due to the intra-moleuclar crosslinked reactions, the other reason is that the large excess unreacted free borate ions and free Na^+ ions act like excess salt and shield the electrostatic charge of PVA–borate complexations. In the present study, the concentration of borax is kept at a fixed value, i.e. [borax]=0.2 M, and the PVA concentration is increased from 2 to 60 g/L. As PVA concentration is increased, more and more borate ions are bound on PVA and form negative charged complexations and more Na^+ ions act as counter-ions rather than free ions. Thus the excess free borate ions and free Na^+ ions decrease as PVA concentration is increased, and the reduction of PVA–borate complexations sizes due to electrostatic shielding of free Na^+ ions on negative charges of PVA–borate complexation decreases while PVA concentration is increased. At 9 g/L≤[PVA]≤15 g/L, both intra- and inter-molecular borate–PVA diol crosslink reactions might happen, and both fast and slow mode relaxations are observed in Fig. 2, indicating that both single PVA molecular chains and PVA aggregated particles are present in the solutions. The fast mode relaxation time, τ_f, increases as PVA concentration is increased from 2 to 15 g/L could be due to the less shielding of free Na^+ ions on negative charged PVA–bortae complexations. At [PVA]=15 g/L, an additional big relaxation peak appears at the shortest relaxation time around log τ=1.7 μs, which may be due to collective relaxation of molecular segments between two neighboring crosslinks or chain overlap points. At [PVA]=20 g/L, DLS data show only slow mode relaxation, indicating that most of the PVA molecules form clusters through borate–PVA diol inter-molecular crosslink reactions.

Fig. 3 shows the plots of fast mode relaxation rate $1/\tau_f$ versus $\sin^2\theta/2$ for 15 g/L PVA solutions mixed with 0.0 and 0.2 M borax. These data show a very good $\sin^2\theta/2$ linear dependency of $1/\tau_f$, suggesting a diffusive process of the fast mode relaxation. Similar fast relaxation mode behavior was also observed for PVA aqueous solutions with 2 g/L≤[PVA]≤60 g/L and PVA–borax aqueous solutions with 2 g/L≤[PVA]≤20 g/L and [borax]=0.2 M. Fig. 4 shows the plots of slow mode relaxation rate $1/\tau_s$ versus

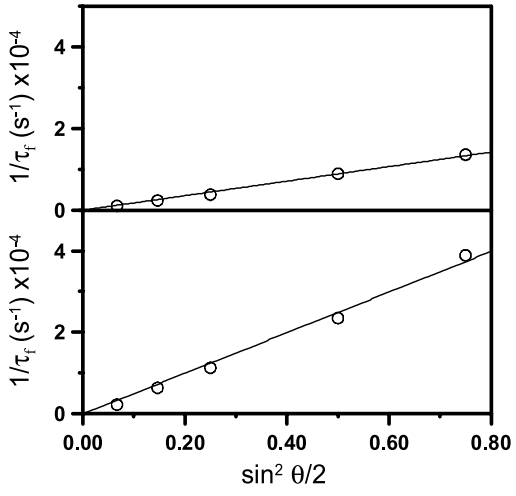

Fig. 3. Plot of $1/\tau_f$ versus $\sin^2\theta/2$ for 15 g/L PVA aqueous solutions mixed with 0.0 M borax (top) and 0.2 M borax (bottom).

$\sin^2\theta/2$ for 20 g/L PVA aqueous solutions mixed with 0.0 and 0.2 M borax. The $1/\tau_s$ data of Fig. 4 are also plotted against $\sin^3\theta/2$ and are shown in Fig. 5. Comparing the linear fitting of Fig. 4 with that of Fig. 5, we found that $1/\tau_s$ had a better $\sin^3\theta/2$ dependency than a $\sin^2\theta/2$ dependency. Similar angular dependency of slow mode $1/\tau_s$ was also observed for other PVA aqueous solutions and PVA–0.2 M borax aqueous solutions with [PVA] $\leq$ 20 g/L. These results suggest that in these solutions the aggregated particles may not overlap with each other and the slow mode relaxation process is more close to an intra-particle motion rather than a diffusion motion.

For PVA–0.2 M borax aqueous systems with [PVA] $\geq$ 40 g/L, the inter-molecular crosslink reactions through borate–PVA di-diol and PVA –OH hydrogen bonds cause the sizes of PVA–boarx particles go to infinity and the PVA–0.2 M borax aqueous systems to behave like gels. The well fit of $g^{(1)}(t)$ data to Eq. (7) reveal a power law behavior of $g^{(1)}(t)$ (Fig. 2). As shown in Table 1, the exponent b of PVA–0.2 M borax aqueous solution with [PVA] = 20 g/L is around 0.53 leading to fractal dimension $d = 0$, indicating a system near but below sol–gel transition. The exponent b decreases from 0.37 to 0.11 and the fractal dimension d increases from 0.26 to 0.78 as PVA concentration increases from 40 to 60 g/L, indicating an increase of crosslink density with increasing PVA concentration. The power law behavior had also been reported in other systems, such as $d = 0.73$ for silica gels prepared in methanol from 1.0 M tetramethoxysilicon (TMOS) with 2.0 M H_2O and 0.1 M NH_3OH base catalyst [32,34], and $d = 0.4$–0.6 for 20 g/L poly(vinyl alcohol) blended with 10–90 mM Congo red thermoreversible gels [33]. Table 1 also shows a decrease of characteristic relaxation time τ as PVA concentration is increased from 40 to 60 g/L. Similar phenomenon of decreasing τ with increasing degree of gelation had also been reported in other systems such as exopolysaccharide–NaCl aqueous [30] and schizophillan/D-sorbitaol aqueous [31] systems. The angular dependency of τ and b for PVA–0.2 M borax aqueous systems with [PVA] $\geq$ 40 g/L had also been investigated in this study, and q-independencies of both τ and b were obtained, indicating a size independent relaxation of these systems. The q-independency of τ and b had also been reported in other systems such as 20 g/L poly(vinyl alcohol) blended with 10–90 mM Congo red gels [33] and schizophyllan-D-sorbitol aqueous gels [31].

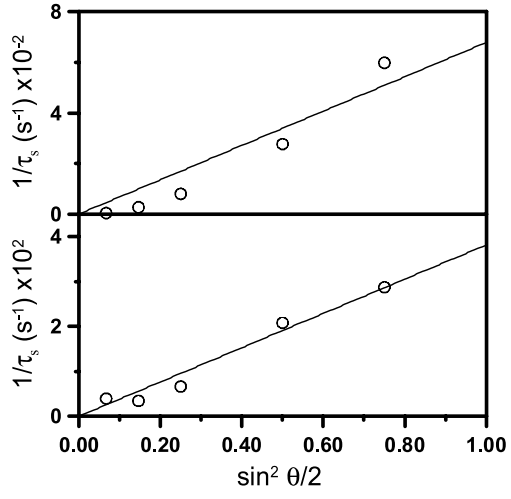

Fig. 4. Plot of $1/\tau_s$ versus $\sin^2\theta/2$ for 20 g/L PVA aqueous solutions mixed with 0.0 M borax (top) and 0.2 M borax (bottom).

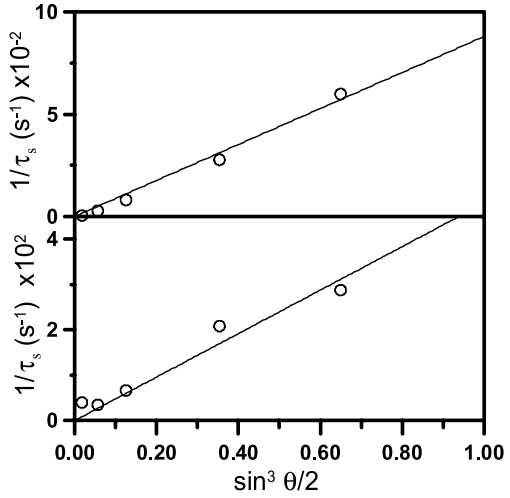

Fig. 5. Plot of $1/\tau_s$ versus $\sin^3\theta/2$ for 20 g/L PVA aqueous solutions mixed with 0.0 M borax (top) and 0.2 M borax (bottom).

Fig. 6 shows the variation of reduced scattered intensity at a scattering angle of 90°, i.e. $\langle I\rangle_T/C$, against sample position for samples with various concentrations of PVA and 0.2 M borax. Where $\langle I\rangle_T$ is the time average intensity, and C the PVA concentration. Each sample, 50 sample points were taken to carry out $\langle I\rangle_T$ measurements. The solid line indicates the ensemble average scattered intensity obtained by averaging $\langle I\rangle_T$ with respect to sample positions. It is known that for a solution $\langle I\rangle_T$ does not depend on sample positions but for a gel $\langle I\rangle_T$ fluctuates strongly with sample position [6,34]. No $\langle I\rangle_T/C$ fluctuation is observed, as PVA concentration is less than 20 g/L. There is a small $\langle I\rangle_T/C$ fluctuation while PVA concentration is at 20 g/L. As PVA concentration is above 40 g/L, $\langle I\rangle_T/C$ fluctuates strongly, suggesting the systems are in gel states.

In order to obtain more information of PVA–borax aqueous solutions, the viscoelastic properties of PVA aqueous solutions in the presence of 0.0, 0.1, and 0.2 M borax were studied using two rheometers. One rheometer (Rheometric Co., model RF-5) with a cone and plate sample holder was used for high viscosity samples measurements (i.e. samples with [PVA] $\geq$ 15 g/L and [borax] $\geq$ 0.1 M). The other was an oscillatory flow rheometer (Vilastic Co., VE system) with a tube sample holder. The oscillatory flow rheometer was used for low viscosity samples measurements (i.e. all PVA aqueous solutions with 0.0 M borax and samples with [PVA] $\leq$ 9 g/L and [borax] $\geq$ 0.1 M).

It has been shown that the gel point of chemical gelation

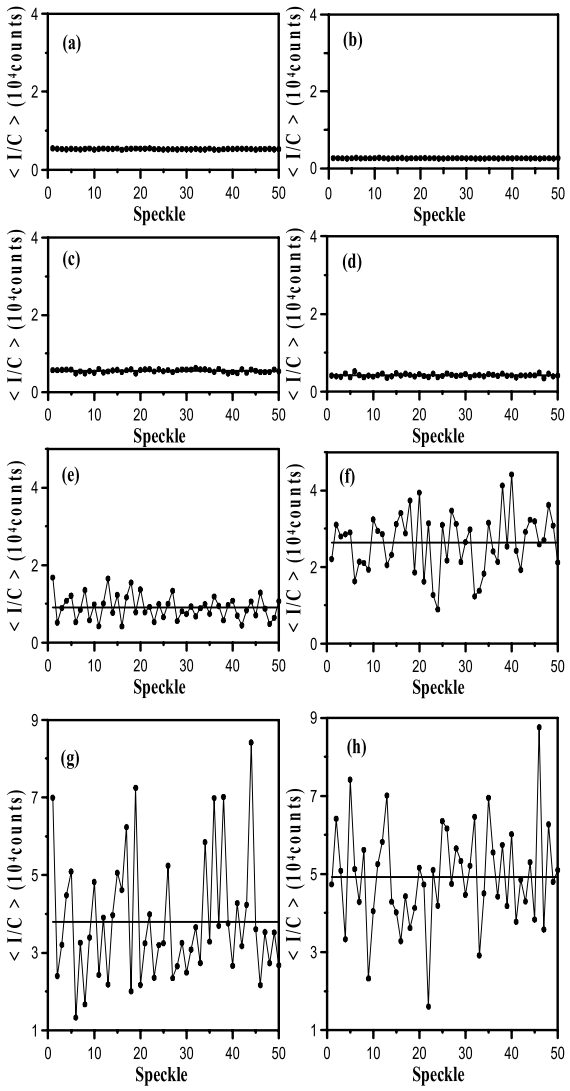

Fig. 6. Reduced scattered intensity $\langle I\rangle_T/C$ against sample position for samples with various concentrations of PVA and 0.2 M borax. Scattering angle $\theta=90°$. PVA concentrations: (a) 2 g/L; (b) 5 g/L; (c) 9 g/L; (d) 15 g/L; (e) 20 g/L; (f) 40 g/L; (g) 50 g/L; (h) 60 g/L.

can be precisely identified and located by Eqs. (3) and (4), with exponents n' and n'' ranging from 0.5 to 0.8 [16,17,35,36]. In contrast to permanent chemical gelation, the transient nature of thermoreversible network junctions make it difficult to study thermoreversible network systems near the gel point. The junctions in thermoreversible networks are formed by secondary forces, such as hydrogen bonds and ionic bonds, and are typically weak enough to be broken by thermal fluctuations. The principal differences between permanent chemical and thermoreversible gels lie in the lifetime and the functionality of the network functions. Chemical bonds are considered to be permanent while the reversible junctions have finite lifetime. From rheological viewpoint, any reversible junctions will be able to release through a relaxation process if the observation time is sufficiently long [29,30,37].

Figs. 7 and 8 are the plots of log $G'(\omega)$ and log $G''(\omega)$ versus frequency log ω for various concentrations of PVA aqueous solutions mixed with 0.0 and 0.2 M borax, respectively. The results of PVA–0.1 M borax aqueous solutions are similar to those of PVA–0.2 M borax aqueous solutions and are not shown in the paper. As shown in Fig. 7, for PVA aqueous solutions without mixing with borax, the value of $G'(\omega)$ at high frequency region ($\omega>50\ s^{-1}$) does not change significantly with PVA concentration. However, value of $G'(\omega)$ at low frequency ($\omega<10\ s^{-1}$) increases with increasing PVA concentration. At [PVA]=40 g/L, the data of $G'(\omega)$ are almost in a linear line. As [PVA]$\geq$50 g/L, there is a plateau around $\omega=6$–$20\ s^{-1}$, indicative of polymer entanglements inside the PVA aggregations. The exponents n' and n'' at $\omega\to0$ are calculated from Fig. 7 and shown in Table 2. Table 2 shows that $n'\sim2.0$ and $n''\sim1.0$ as [PVA]$\leq$15 g/L. Exponent n' decreases from to 1.96 to 1.80 and n'' decreases from 0.97 to 0.85 as PVA concentration increases from 20 to 60 g/L. These results suggest that PVA aqueous solutions are in solution states. Because of

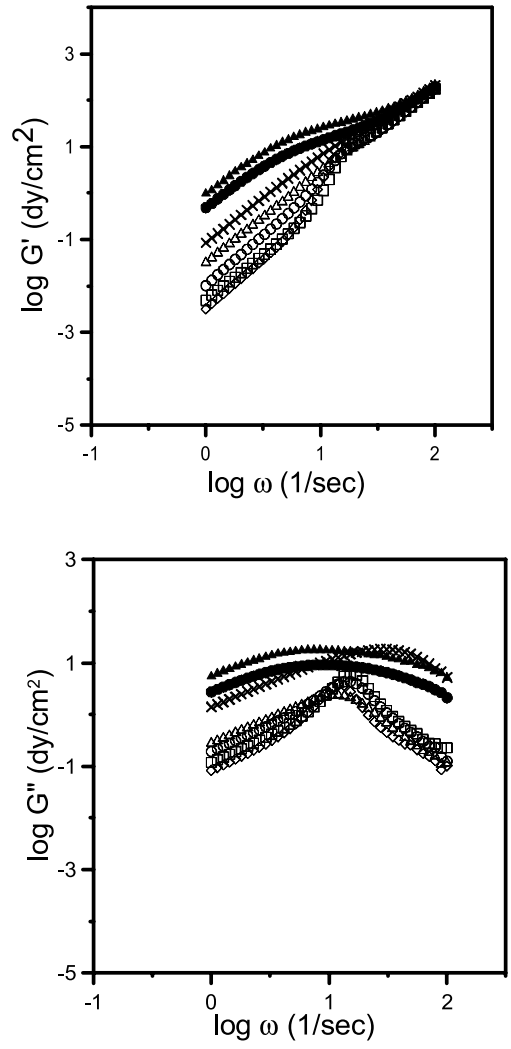

Fig. 7. log $G'(\omega)$ and log $G''(\omega)$ versus log ω of PVA aqueous solutions. [borax]=0.0 M; Concentrations of PVA: (◇) 5 g/L; (□) 9 g/L; (○) 15 g/L; (△) 20 g/L; (×) 40 g/L; (●) 50 g/L; (▲) 60 g/L.

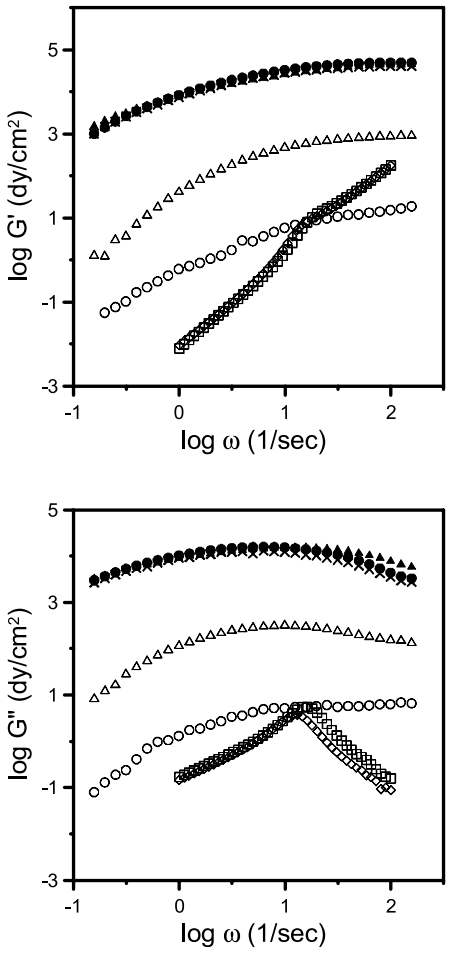

Fig. 8. $\log G'(\omega)$ and $\log G''(\omega)$ versus $\log \omega$ of PVA/borax aqueous solutions. [borax] = 0.2 M; concentrations of PVA: (◇) 5 g/L; (□) 9 g/L; (○) 15 g/L; (△) 20 g/L; (×) 40 g/L; (●) 50 g/L; (▲) 60 g/L.

instrumental limitation, the extremely low viscosity of 2 g/L PVA aqueous solutions causes the anomalous behavior of $G'(\omega)$ and $G''(\omega)$ data. The $G'(\omega)$ and $G''(\omega)$ data of of 2 g/L PVA aqueous solutions mixed with [borax] = 0.0–0.2 M are not shown in Figs. 7 and 8. Their exponents n' and n'' are also not listed in Table 2.

As [borax] ≥ 0.1 M (Fig. 8), we found that the $G'(\omega)$ values of PVA/ water solutions mixed with borax are always higher than those without mixing with borax. Three groups of data can be observed in Fig. 8. (1) [PVA] ≤ 9.0 g/L < C^*, most of the borate/PVA di-diol reactions are intra-PVA molecular reactions, $G'(\omega)$ and $G''(\omega)$ does not change significantly with increasing PVA concentration. (2) $C^* \simeq 15$ g/L ≤ [PVA] ≤ 20 g/L, both borate/PVA di-diol intra- and inter-molecular reactions may happen in this regime, $G'(\omega)$ and $G''(\omega)$ increase with increasing PVA and borax concentrations. There is a plateau of $G'(\omega)$ at $\omega = 10$–$100\ s^{-1}$, indicative of polymer entanglements. (3) $C^* < 40$ g/L ≤ [PVA] ≤ 60 g/L, inter-molecular crosslinking reactions dominate most of the borate/PVA di-diol reactions. $G'(\omega)$ and $G''(\omega)$ values are controlled by the crosslink density, i.e. by the concentration of borax, but not by PVA concentration. In this regime, we noticed that $G'(\omega)$ and $G''(\omega)$ change slightly with increasing PVA concentration while borax is kept at a constant concentration. However, at a fixed PVA concentration, $G'(\omega)$ and $G''(\omega)$ increase with increasing borax concentration. The exponents n' and n'' of $G'(\omega)$ and $G''(\omega)$, respectively, at $\omega \to 0$ calculated from PVA–borax aqueous solutions are also shown in Table 2. We found that at [borax] = 0.1 M, n' decreases from 2.0 to 1.48 and n'' decreases from 1.0 to 0.87 as PVA concentration is increased from 5 to 60 g/L. Similarly at [borax] = 0.2 M, n' decreases from 2.0 to 0.84 and n'' decreases from 1.0 to 0.61 as PVA concentration is increased from 5 to 60 g/L. One of the reasons of the decrements of n' and n'' could be due to the increment of the longest relaxation time with increasing PVA concentration, which leads the flow region of G' and G'' to locate out of the angular frequency wiondow measured. The other reason for the decrements of n' and n'' with increasing PVA concentration is due to property of system is getting close to gel-like behavior. Thus, $n' \leq 1.0$ and $n'' \leq 0.80$ as [PVA] ≥ 40 g/L and [borax] = 0.2 M. However, the critical exponent with $n' = n''$ proposed by Winter et al. [16,17] at a sol–gel transition was not observed in the present study. This result is similar to that reported by Robb et al. [22].

Table 2
Exponents and crossover frequency of $G'(\omega)$ and $G''(\omega)$ of PVA/borax aqueous solutions

[PVA] g/L	n'	n''	$\log \omega_c$ (s^{-1})
[borax] = 0.0 M			
5.0	2.10	1.10	1.08
9.0	2.03	1.10	1.18
15.0	2.04	1.06	1.11
20.0	1.96	0.97	0.91
40.0	1.92	0.94	1.27
50.0	1.83	0.85	0.81
60.0	1.80	0.85	0.80
[borax] = 0.1 M			
5.0	2.05	1.03	1.16
9.0	2.02	1.02	1.09
15.0	1.68	0.92	0.67
20.0	1.67	0.90	0.78
40.0	1.59	0.92	0.71
50.0	1.55	0.90	0.65
60.0	1.48	0.87	0.62
[borax] = 0.2 M			
5.0	2.04	1.04	1.06
9.0	2.05	1.01	1.05
15.0	1.52	0.92	0.94
20.0	1.54	0.86	0.74
40.0	1.00	0.76	0.27
50.0	1.04	0.65	0.26
60.0	0.84	0.61	0.26

The crossover frequency ω_c, is the frequency at which $G'(\omega)$ and $G''(\omega)$ intersect with each other with $G'' > G'$ for $\omega < \omega_c$ and $G' > G''$ for $\omega > \omega_c$. Since the borate–didiol complexation crosslink is a thermal equilibrium crosslink bond with a finite lifetime τ_{life}. As the observation period of viscoelastic measurements is longer than τ_{life} of network

junctions, i.e. $1/\omega > \tau_{life}$, the PVA–borax–water system behaves like a flow liquid medium, i.e. $G'' > G'$. However, as $1/\omega < \tau_{life}$, PVA–borax–water system behaves like a network structure with $G' > G''$. Thus at $\omega > \omega_c$, PVA–borax–water system behaves like a gel medium, but at $\omega < \omega_c$ the system behaves like a flow medium. The crossover frequencies log ω_c are also summarized in Table 2. As PVA concentration is increased from 2 to 60 g/L, log ω_c shifts from 1.07 to 0.62 s^{-1} while borax concentration was 0.1 M, and log ω_c shifted from 1.08 to 0.26 s^{-1} while borax concentration was 0.2 M. These results suggest that the frequency range of observing fluid-like structure ($G' < G''$) decreases as PVA concentration increases. The critical exponent with $n' = n''$ proposed by Winter et al. at a sol–gel transition will cause the curve of log $G'(\omega)$ versus log ω parallel to that of log $G''(\omega)$ versus log ω over the whole frequency for a PVA–borax aqueous solution and thus no crossover frequency ω_c can be observed. The presence of crossover frequency log ω_c of log G' with log G'', as shown in Table 2, suggests that the gel-like behavior was not observed by the pertubing rheometric method in the present PVA–borax aqueous solutions.

4. Conclusion

While [PVA] < 40 g/L with [borax] ≤ 0.2 M and [PVA] ≤ 60 g/L with [borax] = 0.0 M, our DLS, SLS, and dynamic viscoelasticity measurements showed that PVA/borax aqueous system was in a solution state. While 40 g/L ≤ [PVA] ≤ 60 g/L with [borax] = 0.2 M, our DLS and SLS measures revealed that PVA/borax aqueous solutions were in gel states; however, viscoelastic data revealed that PVA/borax aqueous systems were in solutions states, and no sol–gel transition moduli exponents with $n' = n''$ as that of chemical crosslinked sol–gel transition was observed. The borate–PVA didiol complexation and H-bonds of PVA–OH groups provide the crosslinks of PVA molecules. The crosslinks formed by borate–PVA didiol reactions and H-bonds among PVA–OH groups are in a reversible equilibrium state. The reversible equilibrium crosslinks have finite lifetimes, leading to a weak gel behavior of PVA–borax aqueous system. In present work, we showed that non-perturbing light scattering is a better technique than pertubing nature rheometer for investigating reversible crosslink gels.

Acknowledgements

The authors would like to acknowledge the financial support from the National Science Foundation of ROC through grant NSC 87-2216-155-001.

References

[1] Sakurada I. Polyvinyl alcohol fibers. New York: Marcel Dekker; 1985.
[2] Ochiai H, Kurita Y, Murakami I. Makromol Chem 1984;185:167–72.
[3] Sinton S. Macromolecules 1987;20:2430–41.
[4] Shibayama M, Adachi M, Ikkai F, Kurokawa H, Sakurai S, Nomura S. Macromolecules 1993;26:623–7.
[5] Ikkai F, Shibayama M, Nomura S, Han CC. J Polym Sci, Polym Phys Ed 1996;34:939–45.
[6] Tsujmoto M, Shibayama M. Macromolecules 2002;35:1342–7.
[7] Conway MW, Almond SW, Broscoe JE, Harris LE. J Pet Technol 1983;35:315–9.
[8] Pezron E, Leibler L, Ricard A, Lafuma F, Audebert R. Macromolecules 1989;22:1169–74.
[9] Pezron E, Leibler L, Ricard A, Lafuma F, Audebert R. Macromolecules 1988;21:1121–5 [see also p. 1126–1131].
[10] Leibler L, Pezron E, Pincus PA. Polymer 1988;29:1105–9.
[11] Kurokawa H, Shibayama M, Ishimaru T, Nomura S, Wu WL. Polymer 1992;33:2182–8.
[12] Keita G, Ricard A, Audebert R, Pezron E, Leibler L. Polymer 1995; 36:49–54.
[13] Shibayama M, Takeshi T, Nomura S. Macromolecules 1994;27: 5350–8.
[14] Lin HL, Yu TL, Cheng CH. Colloid Polym Sci 2000;278:187–94.
[15] Koike A, Nemoto N, Inoue T, Osaki K. Macromolecules 1995;28: 2339–44.
[16] Winter HH, Chambon F. J Rheol 1987;31:683–97.
[17] Winter HH. Polym Eng Sci 1987;27:1698–702.
[18] Winter HH, Morganelli P, Chambon F. Macromolecules 1988;21: 532–5.
[19] Izuka A, Winter HH, Hashimoto T. Macromolecules 1992;25: 2422–88.
[20] Muthukumar M, Winter HH. Macromolecules 1986;19:1284–5.
[21] Cheng ATY, Rodridguez F. J Appl Polym Sci 1981;26:3895–908.
[22] Robb ID, Smeulders JBAF. Polymer 1997;38:2165–9.
[23] Kjoniksen AL, Nystrom B. Macromolecules 1996;29:5215–22.
[24] Joosten JGH, McCarthy JL, Pusey PN. Macromolecules 1991;24: 6690–9.
[25] Horkay F, Burchaard W, Hecht AM, Geissler E. Macromolecules 1993;26:3375–80 [see also p. 4203–4207].
[26] Horkay F, Burchard W, Geissler E, Hecht AM. Macromolecules 1993; 26:1296–303.
[27] Provencher SW. Makromol Chem 1979;180:201–7.
[28] Kjoniksen AL, Nystrom B. Macromolecules 1996;29:7116–23.
[29] Lang L, Burchard W. Macromolecules 1991;24:814–5.
[30] Coviello T, Burchard W. Macromolecules 1992;25:1011–2.
[31] Fuchs T, Richtering W, Burchard W, Kajiwara K, Kitamura S. Polym Gels Networks 1997;5:541–59.
[32] Martin JE, Wilcoxon J, Odinek J. Phys Rev 1991;A43:858–72.
[33] Tsujimoto M, Shibayama M. Macromolecules 2002;35:1342–7.
[34] Motonaga T, Shibayama M. Polymer 2002;42:8925–34.
[35] Chambon F, Winter HH. Polym Bull 1985;13:499–504.
[36] Chambon F, Petrovic Z, Macknight WJ, Winter HH. Macromolecules 1986;19:2146–9.
[37] Schurtenberger P, Scartazzini R, Luisi PL. Rheol Acta 1989;28: 372–81.